International Research Journal of Engineering and Technology (IRJET) e-ISSN: 2395-0056
Volume: 05 Issue: 09 | Sep 2018 www.irjet.net p-ISSN: 2395-0072

ANALYSIS OF ACTIVE POWER CONTROL TECHNIQUES

A.E.ANYALEBECHI[1], B. O. ANYAKA[2]

[1]*Electrical Engineering Department,Nnamdi Azikiwe University Awka, Anambra State, Nigeria.*
[2]*Electrical Engineering Department, University Of Nigeria Nsukka,Enugu State, Nigeria.*

Abstract:- This paper presents active power control techniques on the Nigeria grid. The performance of two basic equipments from the flexible ac transmission systems (FACTS) family—thyristor controlled series compensator (TCSC) and static phase shifter (SPS)—are analyzed here.A sample data of a particular network bus voltage and phase amgles under both schemes was used. At 50% of the transmission line inductive reactance SPS delivered more than 100KW while TCSC scheme was able to deliver only about 90KW.

Keywords: *TCSC, SPS, FACTS, power flow control, Newton's algorithm.*

1. INTRODUCTION

Electric power consumption has increased tremendously in the last few decades. This demands continuous improvement in energy generation, transmission and distribution efficiency. However, installing new power plants and transmission lines are not the immediate solutions because installation may take several years. In this issue, FACTS technology will provide a promising solution. Installing the FACTS devices in the transmission lines will improve the transmission efficiency and this will improve the stability of the system [1, 2, 3, 4, 5, and 6].

The main objective of this study is to demonstrate the electric power regulatory capabilities of two basic schemes of the FACTS family: the thyristor controlled series compensator and the static phase shifter.

However, the steady state operating condition can as well be determined by finding out the flow of active and reactive power throughout the network and the voltage magnitudes and phase angles at all nodes of the network. The planning and daily operation of modern power systems call for numerous power flow studies. Such information is used to carry out security assessment analysis, where the nodal voltage magnitudes and active and reactive power flows in transmission lines and transformers are carefully observed to assess whether or not they are within prescribed operating limits.

2. FACTS EQUIPMENT REPRESENTATION IN POWER FLOWS

Until very recently, with the exception of the static var compensator (SVC), all plant components used in high-voltage transmission to provide voltage and power flow control were equipment based on electro-mechanical technology, which severely impaired the effectiveness of the intended control actions, particularly during fast changing operating conditions [7]. This situation has begun to change; building on the operational experience afforded by the many SVC installations and breakthroughs in power electronics valves and their control, a vast array of new power electronics-based controllers has been developed. Controllers used in high-voltage transmission are grouped under the heading of FACTS [8] and those used in low-voltage distribution under the heading of Custom Power [9]. The most prominent equipment and their main steady state characteristics relevant for power flow modeling are discussed below.

2a) THE THYRISTOR CONTROLLED SERIES COMPENSATOR (TCSC)

The thyristor controlled series compensator (TCSC) varies the electrical length of the compensated transmission line with little delay. Owing to this characteristic, it may be used to provide fast active power flow regulation. It also increases the stability margin of the system and has proved very effective in damping sub-synchronous resonance (SSR) and power oscillations [10]. The TCSC power flow model presented in this paper is based on the concept of a non-linear series reactance, which is adjusted using Newton's algorithm to satisfy a specified active power flow across the variable reactance representing the TCSC [11]. The schematic representation of the TCSC and its equivalent circuit are shown in Figure (1).

The active power transfer P_{lm} across an impedance connected between nodes l and m is determined by the voltage magnitudes $|V_l|$ and $|V_m|$, the difference in voltage phase angles $\theta_l$and θ_m and the transmission line resistance R_{lm} and reactance X_{lm}. In high-voltage transmission lines, the reactance is much larger than the resistance and the following approximate equation may be used to calculate the active power transfer P_{lm}:

$$P_{lm} = \frac{|V_l||V_m|}{X_{lm}} \sin(\theta_l - \theta_m) \dots\dots (1)$$

If the electrical branch is a TCSC controller as opposed to ordinary transmission line then P_{lm} is calculated using the following expression

$$P_{lm}^{reg} = \frac{|V_l||V_m|}{X_{TCSC}} \sin(\theta_l - \theta_m) \dots\dots (2)$$

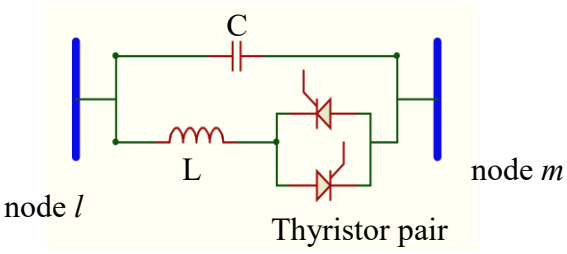

Fig.(1a) TCSC structure formed by fixed capacitor and TCR.

With regard to figure (1a) above, assuming that active power is flowing from node *l* to node m, the effective reactance across the thyristor branch X_{tcr} (and by extension between node *l* and node m, X_{tcsc}) is determined by the firing angles of the thyristors. At low loads the firing angles are reduced thereby increasing the electrical length of the transmission line and hence reducing amount of active power delivered to node m. At high loads the firing angles are also increased thereby shortening the electrical length of the transmission line and hence increasing the amount of active power being delivered. Equations (3) and (4) give mathematical expressions of these scenarios. Figure (1b) is an equivalent circuit of figure (1a) showing X_{tcsc} as a variable reactance.

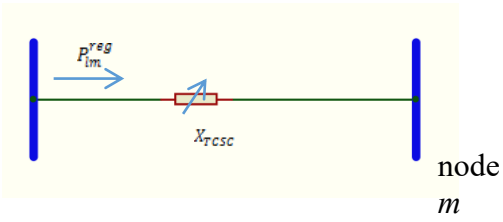

Fig.(1b) TCSC equivalent variable reactance representation.

With regards to figure (1a) the resultant TCSC impedance is obtained using the formula:

$$X_{tcr} = \omega L \left[\frac{\pi}{\sigma - \text{Sin}(\sigma)}\right] \dots\dots\dots (3)$$

and

$$X_{tcsc} = \frac{X_{tcr}.X_C}{(X_{tcr}+X_C)} \dots\dots\dots (4)$$

Where X_{TCSC} is the equivalent reactance of the TCSC controller which may be adjusted to regulate the transfer of active power across the TCSC, hence, P_{lm} becomes P_{lm}^{reg}.

Note, σ = 2β and β = π – α. Also σ is the conducting angle; α is the firing angle; β is the angle of advance.

2 b) TCSC POWER FLOW MODELLING

For inductive operation the TCSC power equations at node *l* are:

$$P_l = \frac{|V_l||V_m|}{X_{TCSC}} \sin(\theta_l - \theta_m) \dots\dots (5)$$

$$Q_l = \frac{|V_l|^2}{X_{TCSC}} - \frac{|V_l||V_m|}{X_{TCSC}} \cos(\theta_l - \theta_m) \dots (6)$$

For capacitive operation, the signs of the equations are reversed. Also, for the power equations corresponding to node m the subscripts *l* and m are exchanged in equations (5)-(6).

For the case when the TCSC is controlling active power flowing from nodes *l* to m at a value P_{lm}^{reg} the set of linearized power flow equations are:

$$\begin{bmatrix} \Delta P_l \\ \Delta P_m \\ \Delta Q_l \\ \Delta Q_m \\ \Delta P_{lm} \end{bmatrix} = \begin{bmatrix} \frac{\partial P_l}{\partial \theta_l} & \frac{\partial P_l}{\partial \theta_m} & \frac{\partial P_l}{\partial |V_l|} & \frac{\partial P_l}{\partial |V_m|} & \frac{\partial P_l}{\partial X_{TCSC}} \\ \frac{\partial P_m}{\partial \theta_l} & \frac{\partial P_m}{\partial \theta_m} & \frac{\partial P_m}{\partial |V_l|} & \frac{\partial P_m}{\partial |V_m|} & \frac{\partial P_M}{\partial X_{TCSC}} \\ \frac{\partial Q_l}{\partial \theta_l} & \frac{\partial Q_l}{\partial \theta_m} & \frac{\partial Q_l}{\partial |V_l|} & \frac{\partial Q_l}{\partial |V_m|} & \frac{\partial Q_l}{\partial X_{TCSC}} \\ \frac{\partial Q_m}{\partial \theta_l} & \frac{\partial Q_m}{\partial \theta_m} & \frac{\partial Q_m}{\partial |V_l|} & \frac{\partial Q_m}{\partial |V_m|} & \frac{\partial Q_m}{\partial X_{TCSC}} \\ \frac{\partial P_{lm}}{\partial \theta_l} & \frac{\partial P_{lm}}{\partial \theta_m} & \frac{\partial P_{lm}}{\partial |V_l|} & \frac{\partial P_{lm}}{\partial |V_m|} & \frac{\partial P_{lm}}{\partial X_{TCSC}} \end{bmatrix}$$

$$= \begin{bmatrix} \Delta\theta_l \\ \Delta\theta_m \\ \Delta V_l \\ \Delta V_m \\ \Delta X_{TCSC} \end{bmatrix} \dots\dots (7)$$

The active power flow mismatch equation in the TCSC is:

$$\Delta P_{lm} = P_{lm}^{reg} - P_{lm}^{calc} \dots\dots\dots (8)$$

And the state variable X_{TCSC} of the series controller is updated at the end of iteration (r) using the following equation

$$X_{TCSC}^{(r+1)} = X_{TCSC}^{(r)} + \Delta X_{TCSC}^{(r)} \dots\dots\dots (9)$$

2c) THE STATIC PHASE SHIFTER (SPS)

The static phase shifter varies the phase angles of the line end voltages with little delay. This is achieved by injecting a voltage in quadrature with the line end voltage at the sending end. This equipment may also be used to provide fast active power flow regulation [12].

The power flow model of the static phase shifter presented in this paper is based on the concept of a lossless transformer with complex taps. The control variable is a phase angle, which is adjusted using Newton's algorithm to satisfy a specified active power flow across the lossless transformer representing the static phase shifter [13]. The schematic representation of the SPS and its equivalent circuit are shown in Figure (2).

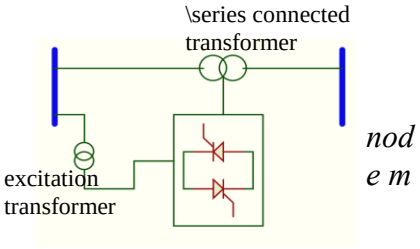

(a)

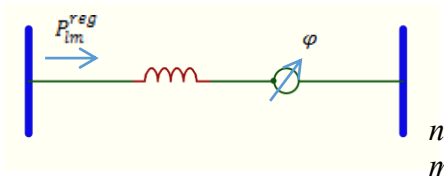

(b)

Fig. (2) SPS: (a) structure formed by a series transformer, an excitation transformer and a network of thyristors; and (b) equivalent variable phase angle representation.

A phase shifting controller with the complex phase angle relationships: $T_v = \cos\varphi + j\sin\varphi$ and $T_I = \cos\varphi - j\sin\varphi$ has the following transfer admittance matrix:

$$\begin{bmatrix} I_l \\ I_m \end{bmatrix} = \frac{1}{X_t}\begin{bmatrix} 1 & -(cos\varphi + jsin\varphi \\ -(cos\varphi - jsin\varphi & 1 \end{bmatrix}\begin{bmatrix} V_l \\ V_m \end{bmatrix} \quad \ldots\ldots\ldots\ldots\ldots\ldots (10)$$

where X_t is the leakage reactance of the series transformer and T_V and T_I are complex tap changing variables related to each other by the conjugate operation. Their magnitude is 1 and their phase angle is φ.

The active power transfer across the phase shifter P_{lm} is calculated using the following expression:

$$P_{lm}^{reg} = \frac{|V_l||V_m|}{X_t}\sin(\theta_l - \theta_m - \varphi) \quad \ldots\ldots\ldots\ldots (11)$$

Suitable adjustment of the phase angle φ enables regulation of active power P_{lm}^{reg} across the phase shifter.

2d). STATIC PHASE SHIFTER POWER FLOW MODELLING

The active and reactive powers injected at node *l* by the SPS shown in Figure (2) are:

$$P_l = |V_l|^2 G_{ll} + |V_l||V_m|(G_{lm}\cos(\theta_l - \theta_m) + B_{lm}\ sin(\theta_l - \theta_m)) \quad \ldots\ldots\ldots (12)$$

$$Q_l = |V_l|^2 B_{ll} + |V_l||V_m|(B_{lm}\cos(\theta_l - \theta_m) - G_{lm}\ sin(\theta_l - \theta_m)) \quad \ldots\ldots\ldots (13)$$

For equations corresponding to node m the subscripts *l* and m are exchanged in equations (12)-(13).

For the case when the SPS is controlling active power flowing from nodes *l* to m at a value P_{lm}^{reg} the set of linearized power flow equations are:

$$\begin{bmatrix} \Delta P_l \\ \Delta P_m \\ \Delta Q_l \\ \Delta Q_m \\ \Delta P_{lm} \end{bmatrix} = \begin{bmatrix} \frac{\partial P_l}{\partial\theta_l} & \frac{\partial P_l}{\partial\theta_m} & \frac{\partial P_l}{\partial|V_l|} & \frac{\partial P_l}{\partial|V_m|} & \frac{\partial P_l}{\partial\Phi} \\ \frac{\partial P_m}{\partial\theta_l} & \frac{\partial P_m}{\partial\theta_m} & \frac{\partial P_m}{\partial|V_l|} & \frac{\partial P_m}{\partial|V_m|} & \frac{\partial P_m}{\partial\Phi} \\ \frac{\partial Q_l}{\partial\theta_l} & \frac{\partial Q_l}{\partial\theta_m} & \frac{\partial Q_l}{\partial|V_l|} & \frac{\partial Q_l}{\partial|V_m|} & \frac{\partial Q_l}{\partial\Phi} \\ \frac{\partial Q_m}{\partial\theta_l} & \frac{\partial Q_m}{\partial\theta_m} & \frac{\partial Q_m}{\partial|V_l|} & \frac{\partial Q_m}{\partial|V_m|} & \frac{\partial Q_m}{\partial\Phi} \\ \frac{\partial P_{lm}}{\partial\theta_l} & \frac{\partial P_{lm}}{\partial\theta_m} & \frac{\partial P_{lm}}{\partial|V_l|} & \frac{\partial P_{lm}}{\partial|V_m|} & \frac{\partial P_{lm}}{\partial\Phi} \end{bmatrix} = \begin{bmatrix} \Delta\theta_l \\ \Delta\theta_m \\ \Delta V_l \\ \Delta V_m \\ \Delta\Phi \end{bmatrix} \quad \ldots\ldots\ldots\ldots\ldots\ldots (14)$$

The active power flow mismatch equation in the SPS is:

$$\Delta P_{lm} = P_{lm}^{reg} - P_{lm}^{calc} \quad \ldots\ldots\ldots\ldots\ldots (15)$$

Equation (11) may be used for the purpose of calculating P_{lm}^{calc} and to derive the relevant Jacobian terms in equation (14). It should be pointed out that the SPS in Figure (2b) has the phase angle tapping in the primary winding and that its effect may be incorporated in the phase angle θ_m. Hence, the Jacobian terms corresponding to P_l, Q_l, P_m, and Q_m are derived with respect to θ_m as opposed to φ, using equations (12) - (13). For cases when the phase shifter angle is in the secondary winding the corresponding Jacobian terms are derived with respect to θ_l.

The state variable φ is updated at the end of iteration (r) using the following equation:

$$\Phi^{(r+1)} = \Phi^{(r)} + \Delta\Phi^{(r)} \quad \ldots\ldots (16)$$

The following table contains data of a standard network:

Table 1: Original network connectivity and Transmission line parameters [14].

Sending node	Receiving node	R (p.u)	X (p.u)	B (p.u)
North	South	0.02	0.06	0.06
North	Lake	0.08	0.24	0.05
South	Lake	0.06	0.18	0.04
South	Main	0.06	0.18	0.04
South	Elm	0.04	0.12	0.03
Lake	Main	0.01	0.03	0.02
Main	Elm	0.08	0.24	0.05

When TCSC was connected at node Lake to control power flow towards node Main the following data was obtained:

Table 2: Nodal complex voltages of a typical TCSC upgraded network [14].

Voltage information	System Nodes North South Lake Main Elm
$\|V\|\ (p.u)$	1.06 1 0.987 0.984 0.972
θ (degrees)	0 -2.04 -4.73 -4.81 -5.7

At 50% of the transmission line inductive reactance given in table 2, the power being delivered to node Main is:

$$P = \frac{(0.987)(0.984)}{0.015} \text{Sin}(-4.73 + 4.81)$$

$$= 0.0904(\text{p.u}) = 90.4\text{KW}$$

At 100% of the transmission line inductive reactance given in table 2, the power being delivered to node Main will be:

$$P = \frac{(0.987)(0.984)}{0.03} \text{Sin}(-4.73 + 4.81)$$

$$= 0.0452(\text{p.u}) = 45.2\text{KW}$$

When the Static Phase Shifter (SPS) replaces the TCSC on the same link between node Lake and node Main the following table was obtained:

Table 3: Nodal Complex voltages of SPS upgraded network [14].

Voltage information	System Nodes North South Lake Main Elm
$\|V\|\ (p.u)$	1.06 1 0.984 0.984 0.97
θ (degrees)	0 -1.77 -5.80 -3.06 -4.95

Using equation (11) let the SPS reactance be 50% 0f the transmission line inductive reactance and the phase shifting angle -2.83.

Therefore,

$$P = \frac{|V_l||V_m|}{X_t} \sin(\theta_l - \theta_m - \varphi)$$

$$= \frac{(0.984)(0.984)}{0.015} \text{Sin}(-5.8 + 3.06 + 2.83)$$

$$= 0.10139(\text{p.u}) = 101.4\text{KW}$$

It should be remarked that the phase shifter achieves phase angle regulation at the expense of consuming reactive power from the network.

Using Newton-Raphson power flow method, the expressions for the active and reactive powers are obtained by representing the complex voltages in polar form, that is

$V_l = |V_l|e^{j\theta_l}$ and $V_m = |V_m|e^{j\theta_m}$. Hence,

$$P_l = |V_l| \sum_{m=1}^{n} |V_m| \{G_{lm} \cos(\theta_l - \theta_m) + B_{lm} sin(\theta_l - \theta_m) \quad (17)$$

$$Q_l = |V_l| \sum_{m=1}^{n} |V_m| \{G_{lm} \sin(\theta_l - \theta_m) + B_{lm} cos(\theta_l - \theta_m) \quad (18)$$

where $|V_l|$ and $|V_m|$ are the nodal voltage magnitudes at nodes l and m while θ_l and θ_m are the nodal voltage phase angles at nodes l and m.

These equations also provide a convenient device for assessing the steady state behaviour of the power network. The equations are non-linear and their solution is reached by iteration. Two of the variables are specified while the remaining two variables are determined by calculation to a specified accuracy. In PQ type nodes two equations are required since the voltage magnitude and phase angle $|V_l|$ and θ_l are not known. The active and reactive powers P_l and Q_l are specified. In PV type nodes one equation is required since only the voltage phase angle θ_l is unknown. The active power P_l and voltage magnitude $|V_l|$ are specified. For the case of the Slack node both the voltage magnitude and phase angle $|V_l|$ and θ_l are specified, as opposed to being determined by iteration. Accordingly, no equations are required for this node during the iterative step.

Equations (17) and (18) can be solved efficiently using the Newton—Raphson method. It requires a set of linearized equations to be formed expressing the relationship between changes in active and reactive powers and changes in nodal voltage magnitudes and phase angles.

The elements of the Jacobian matrix can be found by differentiating equations (17) and (18) with respect to $\theta_l, \theta_m, |V_l| \; and \; |V_m|$.

For the case when l = m:

$$\frac{\partial P_l}{\partial \theta_l} = |V_l| \sum_{m=1}^{n} |V_m| \{-G_{lm} \sin(\theta_l - \theta_m) + B_{lm} cos(\theta_l - \theta_m)\} - |V_l|^2 B_{ll}$$

$$= -Q_l - |V_l|^2 B_{ll} \; \ldots\ldots (19)$$

$$\frac{\partial P_l}{\partial |V_l|} = \sum_{m=1}^{n} |V_m| \{G_{lm} \cos(\theta_l - \theta_m) + B_{lm} sin(\theta_l - \theta_m)\} + |V_l| G_{ll}$$

$$= \frac{P_l}{|V_l|} + |V_l| G_{ll} \; \ldots\ldots\ldots (20)$$

$$\frac{\partial Q_l}{\partial \theta_l} = |V_l| \sum_{m=1}^{n} |V_m| \{G_{lm} \cos(\theta_l - \theta_m) + B_{lm} sin(\theta_l - \theta_m)\} - |V_l|^2 G_{ll}$$

$$= P_l - |V_l|^2 G_{ll} \; \ldots\ldots (21)$$

$$\frac{\partial Q_l}{\partial |V_l|} = \sum_{m=1}^{n} |V_m| \{G_{lm} \sin(\theta_l - \theta_m) - B_{lm} cos(\theta_l - \theta_m)\} - |V_l| B_{ll} = \frac{Q_l}{|V_l|} - |V_l| B_{ll} \; \ldots\ldots (22)$$

For the case when $l \neq m$

$$\frac{\partial P_l}{\partial \theta_m} = |V_l||V_m| \{G_{lm} \sin(\theta_l - \theta_m) - B_{lm} cos(\theta_l - \theta_m)\} \; \ldots\ldots (23)$$

$$\frac{\partial P_l}{\partial |V_m|} = |V_l| \{G_{lm} \cos(\theta_l - \theta_m) + B_{lm} sin(\theta_l - \theta_m)\}$$

$$= -\frac{1}{|V_m|} \frac{\partial Q_l}{\partial \theta_m} \; \ldots\ldots\ldots\ldots (24)$$

$$\frac{\partial Q_l}{\partial \theta_m} = -|V_l||V_m| \{G_{lm} \cos(\theta_l - \theta_m) + B_{lm} sin(\theta_l - \theta_m)\} \; \ldots\ldots (25)$$

$$\frac{\partial Q_l}{\partial |V_m|} = |V_l| \{G_{lm} sin(\theta_l - \theta_m) - B_{lm} cos(\theta_l - \theta_m)\}$$

$$= \frac{1}{|V_m|} \frac{\partial P_l}{\partial \theta_m} \; \ldots\ldots\ldots (26)$$

To start the iterative solution, initial estimates of the nodal voltage magnitudes and phase angles at all the PQ nodes and voltage phase angles at all the PV nodes are given to calculate the active and reactive power injections using equations (17 and 18). Since it is unlikely that the initial estimated voltages will agree with the voltages at the solution point, the calculated power injections will not agree with the known specified powers. The mismatch power vectors may be defined as:

$$\Delta P^{(r)} = (P^{gen} - P^{load}) - P^{calc,(r)} = P^{net} - P^{calc,(r)} \; \ldots (27)$$

$$\Delta Q^{(r)} = (Q^{gen} - Q^{load}) - Q^{calc,(r)} = Q^{net} - Q^{calc,(r)} \; \ldots\ldots (28)$$

The Jacobian elements are then calculated and the linearized equation is solved to obtain the vectors of voltage updates.

$$\boldsymbol{\theta}^{(r+1)} = \boldsymbol{\theta}^{(r)} + \Delta \boldsymbol{\theta}^{(r)} \; \ldots\ldots\ldots\ldots (29)$$

$$|\boldsymbol{V}|^{(r+1)} = |\boldsymbol{V}|^{(r)} + \Delta |\boldsymbol{V}|^{(r)} \; \ldots\ldots (30)$$

The evaluation of equations (17), (18) and the linearized expression as well as (27) - (30) are repeated in sequence until the desired change in power injection (power mismatch) ΔP and ΔQ are within a small tolerance, example $\varepsilon = 10^{-12}$.

As the process approaches the solution, convergence becomes more rapid. The figure below gives the overall flow diagram for the power flow Newton—Raphson method:

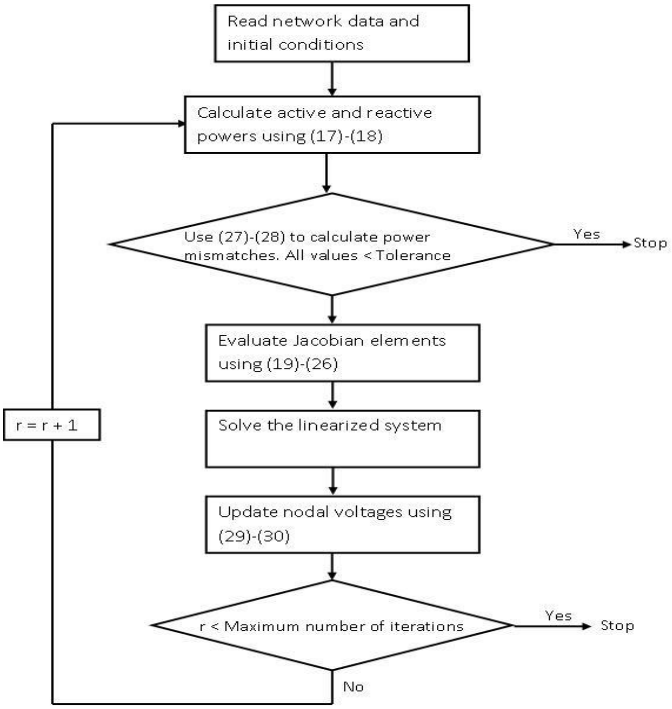

3. CONCLUSION

It is important to state that this study is not about the steady state operation of electric power networks but simply to analyze the regulatory and control capabilities of two basic power control schemes.

Equations (2) and (6) are the mathematical expressions that represent active power flow under the two different schemes. Using the data of a particular sample network, as shown in tables 1, 2 and 3, the active power control capabilities of both schemes were analyzed. At 50% of the transmission line inductive reactance, TCSC scheme was able to deliver about 90.4KW to the next node while SPS scheme was able to deliver about 101.4KW. Again, decreasing the phase shift angle further will tend to increase significantly the active power deliverable by the SPS. Therefore, the SPS scheme is superior to the TCSC scheme in terms of active power control and it is strongly recommended.

4. REFERENCE

[1] A. P. Sangheetha, S. Padma, "Study of Thyristor controlled series compensator for the enhancement of powerflow and stability", International Journal of Scientific & Engineering Research, vol.5, Issue 4, April 2014.

[2] N. H. Hingorani, "Flexible AC transmission systems. "IEEE Spectrum p. 4045, 225-242, Apr. 1993.

[3] R. M. Mathur and R. K. Verma, "Thyristor-based FACTS controllers for electrical transmission systems", IEEE Press, pp 277-288, 2002.

[4] J. V. Kadia, J. G. Jamnani "Modeling and Analysis of TCSC Controller for Enhancement of Transmission Network" International Journal of Emerging Technology and Advanced Engineering Website: www.ijetae.com (ISSN 2250-2459, Volume 2, Issue 3, March 2012) 223

[5] Kusum Arora, S.K. Agarwal, Narendra Kumar, Dharam Vir "Simulation aspects of Thyristor Controlled Series Compensator in Power system" IOSR Journal of Engineering (IOSRJEN) e-ISSN: 2250-3021, p-ISSN: 2278-8719 Vol. 3, Issue 4 (April 2013), IIVII PP 17-26 www.iosrjen.org 17

[6] Khederzadeh, M. "Application of TCSC to enhance Power quality" Universities power Engineering conferences 2007, 42nd International conference, Publication Year: 2007, Page(s): 607-612.

[7] Miller, T.J.E. (ed), *Reactive Power Control in Electric Systems,* John Wiley & Sons, New York, 1982.

[8] Ledu, A., Tontini, G. and Winfield, M., Which FACTS Equipment for Which Need?, *International Conference on Large High Voltage Electric Systems (CIGRE),* Paper 14/37/38-08, Paris, September 1992.

[9] Hingorani, N.G., Flexible AC Transmission Systems, IEEE Spectrum, Vol. 30, No. 4, pp. 41-48, April 1993.

[10] Hingorani, N.G., Introducing Custom Power, IEEE Spectrum, Vol. 32, No. 6, pp. 41-48, June 1995.

[11] Larsen, E.V., Bowler, C., Damsky, B. and Nilsson, S., Benefits of Thyristor Controlled Series Compensation, *International Conference on Large High Voltage Electric Systems* (CIGRE), Paper 14/37/38-04, Paris, September 1992.

[12] Fuerte-Esquivel, C.R. and Acha, E., A Newton-Type Algorithm for the Control of Power Flow in Electrical Power Networks, *IEEE Transactions on Power Systems,* Vol. 12, No. 4, pp. 1474-1480, November 1997.

[13] Hingorani,N.G. and Gyugyi,L., *"Understanding FACTS: Concepts and Technology of Flexible AC Transmission System",* The Institute of Electrical and Electronics Engineers, Inc, New York, 2000.

[14] Acha, et al,"Power Electronic Control in Electrical Systems" Rajkamal Electric Press, 2008.